Metabolic and enzymatic engineering approach for the production of 2-phenylethanol in engineered Escherichia coli

Noda, Shuhei ; Mori, Yutaro ; Ogawa, Yuki ; Fujiwara, Ryosuke ; Dainin, Mayumi ; Shirai, Tomokazu ; Kondo, Akihiko

(Citation)
Bioresource Technology,406:130927

(Issue Date)
2024-08

(Resource Type)
journal article

(Version)
Version of Record

Bioresource Technology 406 (2024) 130927

Contents lists available at ScienceDirect

Bioresource Technology

journal homepage: www.elsevier.com/locate/biortech

Metabolic and enzymatic engineering approach for the production of 2-phenylethanol in engineered *Escherichia coli*

Shuhei Noda [a,b,1,*], Yutaro Mori [c,1], Yuki Ogawa [d], Ryosuke Fujiwara [d], Mayumi Dainin [d], Tomokazu Shirai [d], Akihiko Kondo [a,d]

[a] Graduate School of Science, Technology and Innovation, Kobe University, 1-1 Rokkodai, Nada, Kobe 657-8501, Japan
[b] PRESTO, Japan Science and Technology Agency (JST), Saitama 332-0012, Japan
[c] Department of Chemical Science and Engineering, Graduate School of Engineering, Kobe University, 1-1 Rokkodai, Nada, Kobe 657-8501, Japan
[d] Center for Sustainable Resource Science, RIKEN, 1-7-22, Suehiro-cho, Tsurumi-ku, Yokohama, Kanagawa 230-0045, Japan

HIGHLIGHTS

- Engineered *E. coli* produces 1.1 g/L of 2-phenylethanol (2PE) in batch culture.
- Computer-based enzyme evolution increases 2PE production 4.1-fold.
- *ARO10* I544W mutation in *E. coli* enhances phenylpyruvate binding for high 2PE yield.
- 2PE production reaches 2.5 g/L with a glucose yield of 0.16 g/g after 72 h.

GRAPHICAL ABSTRACT

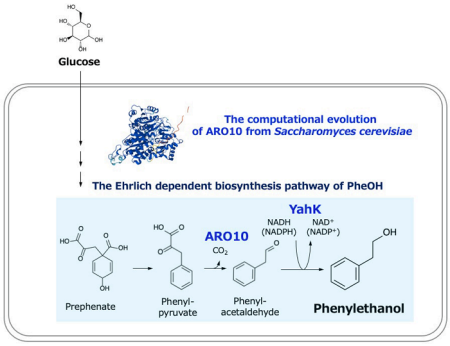

ARTICLE INFO

Keywords:
2-phenylethanol
Phenylpyruvate decarboxylase
Rational design of enzyme
Metabolic engineering

ABSTRACT

2-Phenylethanol, known for its rose-like odor and antibacterial activity, is synthesized via exogenous phenylpyruvate by the sequential reaction of phenylpyruvate decarboxylase (PDC) and aldehyde reductase. We first targeted *ARO10*, a phenylpyruvate decarboxylase gene from *Saccharomyces cerevisiae*, and identified a suitable aldehyde reductase gene. Co-expression of *ARO10* and *yahK* in *E. coli* transformants yielded 1.1 g/L of 2-phenylethanol in batch culture. We hypothesized that there might be a bottleneck in PDC activity. The computer-based enzyme evolution was utilized to enhance production. The introduction of an amino acid substitution in ARO10 (ARO10 I544W) stabilized the aromatic ring of the phenylpyruvate substrate, increasing 2-phenylethanol yield 4.1-fold compared to wild-type ARO10. Cultivation of ARO10 I544W-expressing *E. coli* produced 2.5 g/L of 2-phenylethanol with a yield from glucose of 0.16 g/g after 72 h. This approach represents a significant advancement, achieving the highest yield of 2-phenylethanol from glucose using microbes to date.

* Corresponding author.
E-mail address: shuhei.noda@opal.kobe-u.ac.jp (S. Noda).
[1] Contributed equally to this work.

https://doi.org/10.1016/j.biortech.2024.130927
Received 5 March 2024; Received in revised form 24 May 2024; Accepted 31 May 2024
Available online 1 June 2024

1. Introduction

Metabolic engineering research has developed significantly over the last few decades. Researchers have designed and constructed metabolic pathways to produce compounds of interest using genetically engineered microbes (Lu et al., 2019; Nielsen, 2019; Choi et al., 2020; Jovanovic et al., 2021; Otero-Muras and Carbonell, 2021). The development of metabolic engineering is closely related to that of enzymatic and genetic engineering, which are important tools for constructing metabolic pathways in microorganisms. Directed enzyme evolution by random mutagenesis coupled with screening has been widely implemented (Bloom et al., 2005; Machado et al., 2012; Feng et al., 2017; Gao et al., 2022). Recently, the rational design of metabolic enzymes based on computational simulations has been extensively investigated (Li et al., 2018; Antony et al., 2019; Crawshaw et al., 2022; Park et al., 2023). Previously described rationally designed enzymes have enabled researchers to engineer microbes producing unnatural chemicals or compounds of interest at higher yields than previously possible (Weise et al., 2015; Mori et al., 2021). Thus, metabolic and enzymatic engineering has co-evolved.

2-Pheylethanol (2PE) is an industrially valuable aromatic chemical with a rose-like odor and antibacterial activity (Hua and Xu, 2011; Wang et al., 2019). There are numerous reports on the microbial production of 2PE using various microorganisms, such as *Escherichia coli*, *Saccharomyces cerevisiae*, and *Bacillus licheniformis* (Zhan et al., 2022; Wang et al., 2023; Zhu et al., 2023). Several pathways for the synthesis of 2PE have been previously reported. The Ehrlich pathway is well known for producing branched-chain higher alcohols and can be used for 2PE production (Atsumi et al., 2008). When yeast is used as the host strain, the Ehrlich pathway is part of its metabolic pathway, and 2PE is produced from the L-phenylalanine substrate (Chen et al., 2017; Wang et al., 2017; Wang et al., 2018; Gu et al., 2020; Zhu et al., 2021). To produce 2PE from biomass-derived sugars, such as glucose and xylose, the metabolic design of the biosynthesis route via the Ehrlich pathway requires significant changes. After phenylpyruvate is synthesized from these simple sugars via the shikimate pathway, the intermediate is converted into 2PE by a sequential reaction catalyzed by phenylpyruvate decarboxylase (PDC) and aldehyde reductase (ALR). In addition to the Ehrlich pathway-based routes, alternative biosynthetic pathways involving styrene and phenylacetaldehyde have been reported (Machas et al., 2017). Due to its industrial value, the production of 2PE has been thoroughly investigated using various host strains and metabolic pathways.

When considering the microbial production of 2PE, the selection and combination of PDC and ALR are among the most significant factors for achieving higher production. 2PE is naturally synthesized by various yeast species, including *Saccharomyces cerevisiae*. In particular, the gene resources of PDC have generally been derived from yeasts. *ARO10* from *S. cerevisiae* is one of the most widely available PDC genes involved in 2PE production.

The enzyme encoded by the *ARO10* gene was identified as an aromatic 2-keto acid decarboxylase with substrate specificity for phenylalanine, tryptophan, and tyrosine (Vuralhan et al., 2003; Vuralhan et al., 2005; Kneen et al., 2011). The introduction of *ARO10* into host strains has resulted in successful 2PE production by various microorganisms (Wang et al., 2019). In other reports, heterologous expression of 2-ketoisovaleate decarboxylase (Kivd) from *Lactococcus lactis* in *B. licheniformis* led to 2PE production with a higher titer and yield than using other host strains, such as *E. coli* and *S. cerevisiae* (Zhan et al., 2022; Rao et al., 2023). Engineering the host strain to enhance the carbon flux for 2PE production and developing a toolbox for gene expression in *B. licheniformis* have significantly increased 2PE production. When using different host strains such as *E. coli*, *S. cerevisiae*, or *B. licheniformis*, the maximum amount of 2PE produced from glucose was 2.28, 0.41, or 6.95 g/L, respectively (Romagnoli et al., 2014; Wang et al., 2019; Rao et al., 2023). Although metabolic engineering approaches have been widely used for 2PE production, to the best of our knowledge, directed or rational evolution of the enzymes involved in the 2PE biosynthetic pathway has not yet been conducted.

The rational design and creation of metabolic enzymes are powerful tools for manipulating the carbon flux and promoting the production of compounds of interest. Although directed mutagenesis of enzymes combined with random mutagenesis requires a high-throughput screening system to evaluate numerous enzyme mutants, only a limited number of mutant libraries must be investigated for rational enzyme design based on *in silico* computational simulations. Several studies have reported microbial production using this approach for the rational design of metabolic enzymes (Machado et al., 2012; Gao et al., 2022). We also previously demonstrated the possibility of producing 1,3-butadiene using genetically engineered *E. coli* expressing rationally evolved ferulic acid decarboxylase (Mori et al., 2021).

In this study, we used a combination of metabolic and enzymatic-engineering approaches to produce 2PE from engineered *E. coli*. While various microbes have been used to produce 2PE, we chose *E. coli* over *S. cerevisiae*. When using glucose as the carbon source for 2PE production, the carbon flux to the shikimate pathway from glucose is a key factor. Enhancing this pathway in *S. cerevisiae* is difficult due to the strong carbon flux to ethanol via pyruvate. In fact, the maximum amount of 2PE produced from glucose using *S. cerevisiae* was only 0.41 g/L (Romagnoli et al., 2014). Using the CFT3 strain as the host strain, which is an L-phenylalanine-overproducing *E. coli*, the gene set involved in the biosynthetic pathway of 2PE was optimized (Noda et al., 2015). We focused on the *ARO10* gene (a PDC gene) and screened for an ALR suitable for 2PE production in the CFT3 strain. To enhance 2PE production, we applied a computationally rational design method to the evolution of ARO10. We designed ARO10 mutants based on the affinity between ARO10 and phenylpyruvate and their capacity to synthesize 2PE. In CFT3, the substitution of amino acid residues in a putative substrate-binding module within ARO10 resulted in a higher production of 2PE from glucose than that obtained using wild-type ARO10. The 2PE-producing *E. coli* created in this study is a promising strain for the industrial production of 2PE.

2. Materials and Methods

2.1. Strains and plasmid construction

The strains and plasmids used in this study are listed in Table S1. *E. coli* NovaBlue-competent cells (Novagen, Madison, WI, USA) were used for gene cloning. The polymerase chain reaction was performed using KOD FX Neo DNA polymerase (Toyobo, Osaka, Japan) or PrimeSTAR Max DNA polymerase (Takara, Shiga, Japan); the primer pairs are listed in Table S2. Each gene was assembled with the respective plasmids using the NEBuilder HiFi DNA Assembly (New England Biolabs, Ipswich, MA, USA). A detailed description of the plasmid construction process is provided in the Supplementary Methods. The synthetic genes were ordered from Thermo Fisher Scientific Inc. (Life Technologies, Carlsbad, CA, USA) and are summarized in the Supplementary Information. Plasmids were transformed into bacterial strains using a Gene Pulser II (Bio-Rad, Hercules, CA, USA). Where applicable, 100 $\mu g \cdot mL^{-1}$ ampicillin and 15 $\mu g \cdot mL^{-1}$ chloramphenicol were added to the media for selection. The transformants constructed in this study are listed in Table S1. Plasmid pZE12-Ptrc-ARO10 was constructed as follows: The plasmid gene fragment of pZE12-Ptrc was amplified using PCR with pZE12-Ptrc as the template and inv_trc_fw and inv_trc_rv as the primer pairs. The amplified gene fragment and synthetic ARO10 gene were conjugated together, and the resulting plasmid was named pZE12-Ptrc-ARO10. Next, the synthetic ADH1 gene was introduced into the *Hin*dIII site of pZE12-Ptrc-ARO10, and the resulting plasmid was named pZE12-Ptrc-ARO10-ADH1. The pSAK-Ptrc-ARO10-ADH1 plasmid was constructed as previously described. pZE12-Ptrc-ARO10-yahK and pZE12-Ptrc-ARO10-adhA were constructed as follows: The yahK gene

fragment was amplified using PCR with *E. coli* K-12 MG1655 genomic DNA and pZE12-Ptrc-Kivd-adhA as templates, and yahK_hind_fw and yahK_hind_rv as well as adhA_hind_fw and adhA_hind_rv as primer pairs, respectively. The amplified gene fragments were introduced into the *Hin*dIII site of pZE12-Ptrc-ARO10, and the resulting plasmids were named pZE12-Ptrc-ARO10-yahK and pZE12-Ptrc-ARO10-adhA. The pZE12-Ptrc-ARO10-par plasmid was constructed as follows: The synthetic *Par* gene was introduced into the *Hin*dIII site of pZE12-Ptrc-ARO10, and the resulting plasmid was named pZE12-Ptrc-ARO10-par. pTF-DfeaB was constructed as follows: The gene fragment for *feaB* deficiency was amplified using PCR with *E. coli* K-12 MG1655 genomic DNA as the template and the appropriate primer pairs (Table S2). The amplified fragment used for gene deficiency was introduced into the SpeI site of pTargetF, and the resulting plasmid was named pTF-feaB. The pTF-N20ΔfeaB plasmid was constructed as follows: To introduce the N20 sequence into pTF-feaB, the plasmid fragment pTF-N20_ΔfeaB was amplified using PCR with pTF-feaB as the template and inv_n20_feab_fw and inv_n20_feab_rv as the primer pairs (Table S2). The resulting fragment was self-assembled, and the obtained plasmid was named pTF-N20ΔfeaB.

2.2. Inactivation of chromosomal genes

To delete the chromosomal gene *feaB*, the CRISPR-Cas9 two-plasmid system with pTargetF and pCas was used (Chen et al., 2015). Each gene was inactivated using appropriate plasmids derived from pTargetF. The strains and their phenotypes are summarized in Table S1.

2.3. Culture conditions

M9Y medium was used for maleate production in 5-mL test tube-scale cultures. M9Y minimal medium contains (per liter): glucose, 20 g; yeast extract, 5 g; NaCl, 0.5 g; $Na_2HPO_4{\cdot}12H_2O$, 17.1 g; KH_2PO_4, 3 g; NH_4Cl, 2 g; $MgSO_4{\cdot}7H_2O$, 246 mg; $CaCl_2{\cdot}2H_2O$, 14.7 mg; $FeSO_4{\cdot}7H_2O$, 2.78 mg; thiamine hydrochloride, 10 mg; L-tyrosine, 40 mg; and L-tryptophan, 40 mg (Tyr and Trp were included because CFT3 is auxotrophic for these amino acids). For culturing the CFT3 derivative strains, 10 mM sodium pyruvate was added to the medium to encourage bacterial growth in the initial phase. When needed, ampicillin or chloramphenicol was added to the medium to a final concentration of 100 and 15 $\mu g{\cdot}mL^{-1}$, respectively. Each pre-culture was seeded in 5 mL M9Y medium in a test tube at an initial OD_{600} of 0.05. Tube-scale cultures were incubated at 37 °C in a shaker at 180 rpm. 0.1 mM of isopropyl β-D-thiogalactopyranoside (IPTG) was added to the culture medium at an OD_{600} of 0.5.

Product yield was calculated as Yield ($g{\cdot}g^{-1}$) = [produced compound, g]/[consumed glucose, g].

2.4. Analytical methods

Cell growth was monitored by measuring the OD_{600} using a UVmini-1240 spectrophotometer (Shimadzu, Kyoto, Japan). The glucose concentration in the culture supernatant was measured using the Glucose CII test (Wako, Kyoto, Japan) following the manufacturer's protocol. GC–MS analyses were conducted as follows. To estimate the produced Phe yield, GC–MS was performed using a GCMS-QP2010 Ultra system (Shimadzu, Kyoto, Japan) equipped with a CP-Sil 8 CB-MS capillary column (30 mx0.25 mmx0.25 μm; Agilent). Helium was used as the carrier gas to maintain a flow rate of 2.1 mL/min. The injection volume was 1 μL, with a split ratio of 1:10. The oven temperature was initially held at 150 °C for 5 min, raised to 300 °C at 10 °C/min, and then held at 300 °C for 5 min. The total running time was 25 min. The other parameters were set as follows: 250 °C interface temperature, 200 °C ion-source temperature, and electron impact ionization (EI) at 70 eV. Dried Phe residues were derivatized for 60 min at 80 °C in 30 μL *N*-(*tert*-butyldimethylsilyl)-*N*-methyl-trifluoroacetamide (MTBSTFA) and 30 μL *N*,*N*-dimethylformamide prior to analysis. Cycloleucine was used as an internal standard. To estimate the produced 2PE yield, GC–MS was again performed using GCMS-QP2010 Ultra (Shimadzu, Kyoto, Japan) but equipped with a Pure-WAX (32 m × 0.25 mm × 0.25 μm) column (GL Sciences, Japan). Helium was used as the carrier gas to maintain a flow rate of 2.1 mL/min. The injection volume was 1 μL, with a split ratio of 1:10. The oven temperature was raised from 50 °C to 200 °C at 20 °C/min. The total running time was 7.5 min. The other parameters were set as follows: 200 °C interface temperature, 200 °C ion-source temperature, and EI at 70 eV. Isopropanol was used as an internal standard.

2.5. ARO10 activity assay using lysate

The strains were pre-cultured in 5 mL of M9Y medium supplemented with 10 mM sodium pyruvate and 100 μg/mL ampicillin at 37 °C overnight in a shaker at 180 rpm. Each pre-culture was transferred to 50 mL of the same M9Y medium in a flask with an initial OD_{600} of 0.05. Flask cultures were incubated at 37 °C in a shaker at 180 rpm for 24 h. IPTG (0.1 mM) was added to the culture medium at an OD_{600} of 0.5. The cell pellet was washed twice using phosphate-buffered saline. Cells were sonicated after resuspending in 100 mM potassium phosphate buffer with 1 mM $MgSO_4$ and 0.5 mM ThDP. The cell solution was centrifuged at 15,000 × g for 20 min at 4 °C, and the resulting supernatant was used as lysate for the enzyme activity assay. Absorbance at 280 nm was measured to determine the total amount of protein in the lysate. The reaction mixture included 1 mM $MgSO_4$, 0.5 mM ThDP, 2 mM NADH, 0.25 μM to 10 mM phenylpyruvate, 0.5 mg/mL lysate, and KH_2PO_4/K_2HPO_4 (pH 7.0).

2.6. Homology modeling of ARO10 and in silico mutagenesis

Homology models of ARO10 were generated using MOE (Molecular Operating Environment software, version 2019.01), with the crystal structure of pyruvate decarboxylases from *S. cerevisiae* (PDB: 2VK8) as a template. For homology modeling, the force field of AMBER10, extended Hückel theory (EHT) force field, and implicit solvation model of the reaction field (Born 1:80; cutoff 8,10) were selected, and a thiamine diphosphate (ThDP) molecule in 2VK8 was used as the environment.

To construct a model of ARO10 and obtain phenylpyruvate, the crystal structure of phenylpyruvate decarboxylase from *Azospirillum brasilense* (PDB:2Q5O) was superimposed on the model of ARO10, and the crystal structure was deleted, except for phenylpyruvate from 2Q5O. The model was subsequently protonated using the protonate3D tool at a pH of 7.0 and a temperature of 300 K. Next, the model was optimized by energy minimization using the AMBER10:EHT force field (gradient = 0.01 RMS kcal/mol A^{-2}).

The residue scan tool of MOE was used for *in silico* mutation analysis of ARO10 containing phenylpyruvate and ThDP, with the following settings: residues, V289, M290, N307, E334, I335, T444, F449, L469, I544, I548, L621, V625, and A628; mutations, alanine, glycine, leucine, isoleucine, methionine, phenylalanine, tryptophan, tyrosine, and valine; site limit, 1; affinity atoms, phenylpyruvate. The effect of the mutation on the binding free energy (ΔG_{bind}) between phenylpyruvate and the ARO10 mutants was calculated; the relative binding free affinity changes (Δaffinity) between the ARO10 mutant (ΔG_{mutant}) and ARO10 WT (ΔG_{WT}) were obtained from MOE. Models of multiple ARO10 mutants were generated using the MOE Protein Builder tool.

3. Results and discussion

3.1. 2PE production using ARO10 and ADH1 from S. Cerevisiae in a phenylalanine-overproducing e. Coli CFT3

The biosynthetic pathway of 2PE is initiated by the decarboxylation

of phenylpyruvate into phenylacetaldehyde (Fig. 1). This enzymatic reaction is catalyzed by PDC, which is present in various microbial species. In the production of 2PE using genetically engineered yeasts, PDC derived from *S. cerevisiae*, such as KDC and ARO10, has been widely used with both glucose and L-phenylalanine as substrates. In other reports on 2PE production using prokaryotes as the host strain, KivD and IpdC from *L. lactis* and *A. brasilense*, respectively, were used for the decarboxylation of phenylpyruvate in addition to yeast PDCs.

First, we produced 2PE by overexpressing the genes ARO10 and ADH1 from *S. cerevisiae* in an L-phenylalanine-overproducing *E. coli* CFT3 that we previously created (Noda et al., 2016). The gene set of *ARO10* and *ADH1* was introduced into two different copy-number plasmids, high and low, under the control of the *trc* promoter region. Fig. 2 shows the culture profiles of the 2PE-producing strains. The maximum amount of 2PE produced was 450 mg/L using the culture supernatant of the C3HA10A1 strain, which carries the genes involved in 2PE production and uses a high-copy-number plasmid, after 96 h, whereas C3LA10A1 produced only 220 mg/L of 2PE at the same cultivation time. The maximum cell growth of each strain was similar to that of the 2PE production and glucose consumption, indicating higher cell growth and glucose consumption in C3HA10A1 than in C3LA10A1. However, the initial 2PE production associated with C3LA10A1 cultivation was greater than that associated with C3HA10A1.

During the production of 2PE using yeast as the host strain, the endogenous activity of phenylpyruvate decarboxylase or the introduction of *ARO10* gene from *S. cerevisiae* has been used as a general strategy to synthesize phenylacetaldehyde (Wang et al., 2019). In addition to its use in *E. coli*, *ARO10* is generally known as a promising gene encoding PDCs; however, previous studies reported the use of *kdc* or *ipdC* from *Pichia pastoris* GS115 or *A. brasilense* (Wang et al., 2017). In this study, the production of 2PE reached 450 mg/L with a glucose yield of 0.05 g/g. These values were comparable to those reported in previous studies on 2PE production from glucose using *E. coli* as the host strain (Table S3). In a study on 2PE production using *B. licheniformis*, Zhan et al. (2022) reported a successful titer and yield from glucose. KivD from *L. lactis*, which is famous for its isobutanol production, was used as the PDC in their reports. We also assessed the 2PE produced using KivD. The maximum amount of 2PE produced was 210 mg/L with a yield from glucose of 0.03 g/g after 96 h of cultivation (Fig. S1). These results suggest that ARO10 is a better PDC candidate than KivD, which is opposite to the observations in *B. licheniformis*.

3.2. Optimization of the gene of acetaldehyde reductase combined with *ARO10*

The second step in the 2PE biosynthetic pathway is the conversion of phenylacetaldehyde into 2PE by ALR. This enzyme has numerous varieties, and various enzymes of different origins are available for the production of 2PE in *E. coli* and other prokaryotes (Wang et al., 2019). For 2PE production using *S. cerevisiae*, no additional introduction of genes encoding ALR is necessary as it endogenously produces alcohols (Wang et al., 2019).

In this study, we examined three genes that encode ALR and expressed them with *ARO10* in CFT3 cells. The ALR genes derived from *Rosa x damascena* (*Par*), *L. lactis* (*adhA*), and *E. coli* (*yahK*) were introduced downstream of *ARO10* and evaluated in the CFT3 strain. Fig. 3 shows the culture profiles of the 2PE-producing strains. After 96 h of cultivation, the maximum amount of 2PE produced was 1,130 mg/L in the culture supernatant of the C3HA10yk strain expressing *ARO10* and *yahK*. C3HA10pa and C3HA10ad expressing *Par* and *adhA* with *ARO10* produced 660 and 450 mg/L of 2PE, respectively, after 96 h of cultivation. The yields of 2PE produced from glucose using C3HA10yk, CFT3HA10pa, and CFT3HA10ad after 96 h of cultivation were 0.14, 0.092, and 0.055 g/g, respectively. Cell growth and the amount of glucose consumed by CFT3HA10pa were slightly lower than those of C3HA10yk and C3HA10ad (Fig. 3).

In reports on 2PE production using *E. coli* as the host strain, various types of ALR genes derived from different origins have been adopted,

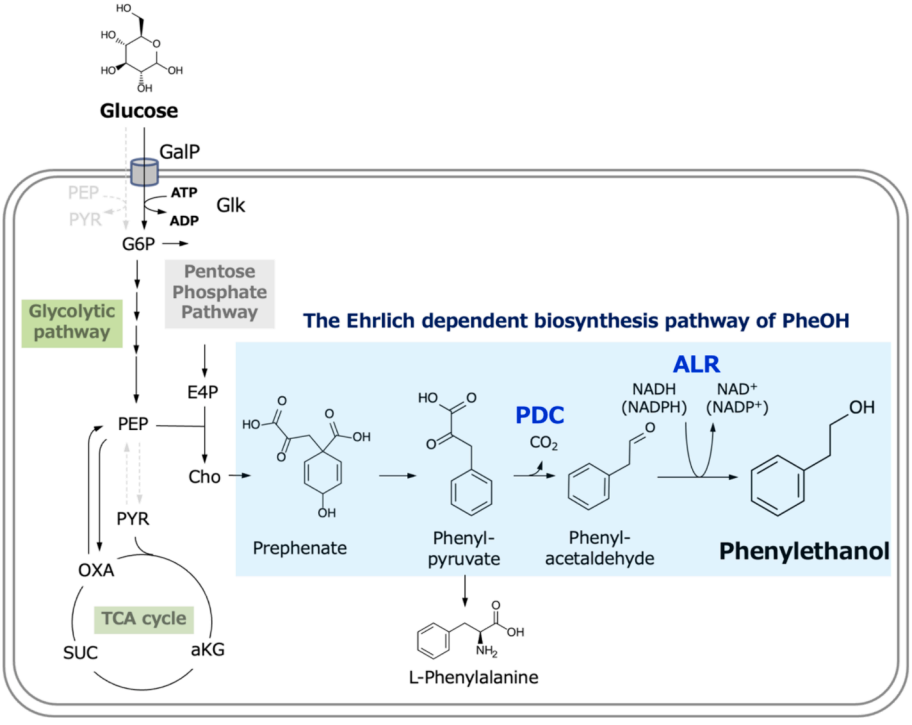

Fig. 1. Metabolic pathway for the production of 2PE from glucose in *E. coli* Abbreviations: Cho, chorismate; DAHP, 3-deoxy-D-heptulosonate-7-phosphate; E4P, erythrose-4-phosphate; G6P, glucose-6-phosphate; NAD^+, oxidized NAD; NADH, reduced NAD; $NADP^+$, oxidized NADP; NADPH, reduced NADP; PEP, phosphoenolpyruvate; PYR, pyruvate; OXA, oxaloacetate; aKG, alpha-ketoglutarate; SUC, succinate; ATP, adenosine triphosphate; ADP, adenosine diphosphate; GalP, galactose permease; Glk, glucokinase.

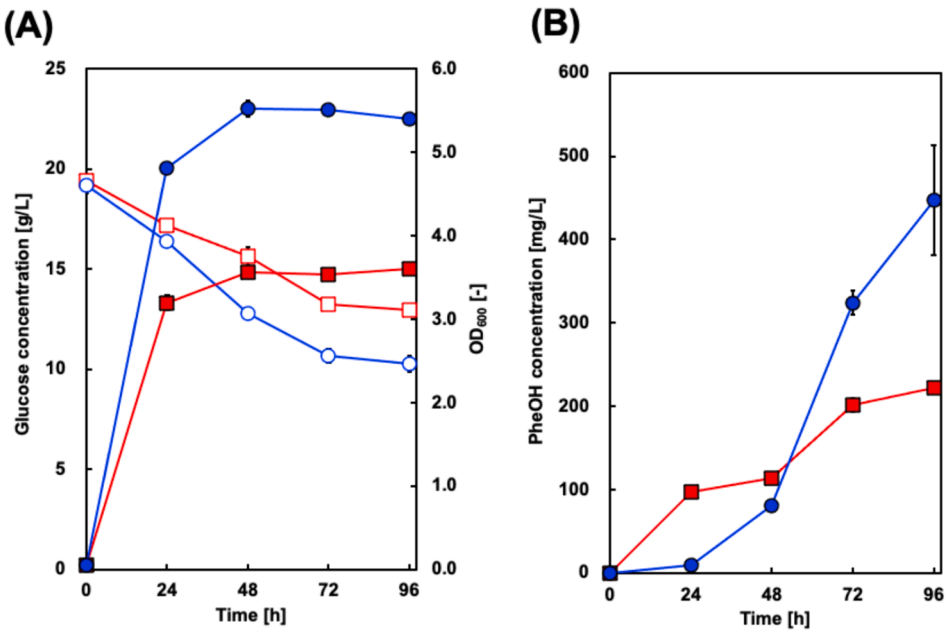

Fig. 2. Culture profiles of 2PE-producing strains using two different plasmids. Time course of (a) OD_{600} values (open symbols) and the amount of consumed glucose (closed symbols), and (b) the amount of produced 2PE in C3HA10A1 (blue symbols) and C3LA10A1 (red symbols). Data are presented as the mean ± standard deviation of three independent experiments. (For interpretation of the references to colour in this figure legend, the reader is referred to the web version of this article.)

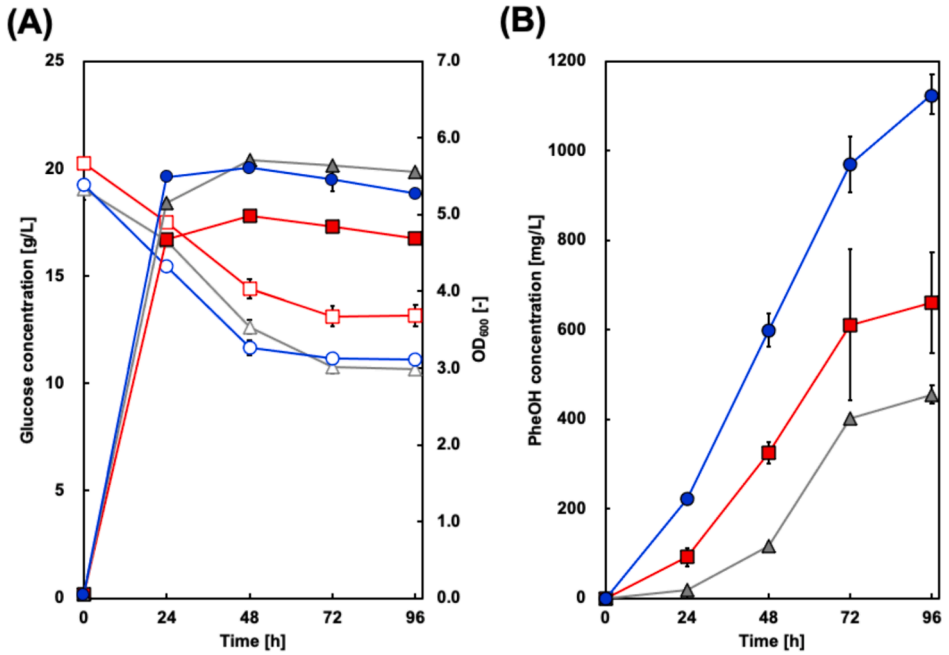

Fig. 3. Culture profiles of 2PE-producing strains using three different ALRs. Time course of (a) OD_{600} values (open symbols) and the amount of consumed glucose (closed symbols), and (b) the amount of produced 2PE in C3HA10yk (blue symbols), C3HA10pa (red symbols), and C3HA10ad (gray symbols). Data are presented as the mean ± standard deviation of three independent experiments. (For interpretation of the references to colour in this figure legend, the reader is referred to the web version of this article.)

whereas endogenous ALR activities were available when yeasts were used (Wang et al., 2019). Several research groups have reported the production of 2PE using YjgB from *E. coli* as an ALR and have overexpressed the gene encoding this endogenous enzyme. To produce 2PE from glucose in *E. coli*, the combined gene set of *ARO10* and *yjgB* was overexpressed. Wang et al. (2023) successfully demonstrated the production of 2PE at a titer of 2.28 g/L using genetically engineered *E. coli* carrying this gene set. However, the yield of 2PE from glucose using *E. coli* expressing *ARO10* and *yjgB* was below 0.10 g/g in each report. Koma et al. (2012) produced 2PE using *E. coli* harboring the *ipdC* and *yahK* gene set, and they obtained a yield from glucose of approximately 0.1 g/g, which was the highest 2PE production yield using *E. coli* as the host strain, although the 2PE titer produced was below 1.0 g/L. In this study, we achieved 2PE production from glucose with titers and yield of 1.1 g/L and 0.14 g/g, respectively. To further enhance the productivity of 2PE, we focused on the competitive carbon flux during the 2PE

production. FeaB is a native NAD^+-dependent phenylacetic acid synthase converting 2-phenylacetaldehyde, the precursor of 2PE, into 2-phenylacetic acid. Here, we created a *feaB*-deficient mutant of CFT3 and introduced it into the gene cluster for 2PE production, followed by an evaluation of the 2PE production using this transformant. Surprisingly, no 2PE production was confirmed in the culture CDfeaBA10yk, whereas the amount of Phe produced reached approximately 1.65 g/L (Fig. S2). In a previous study on 2PE production using engineered *E. coli*, a *feaB*-deficient *E. coli* mutant was used as the base strain. This *E. coli* strain, which possessed a similar genome to our CFT3D*feaB* strain, produced almost 1.1 g/L of 2PE from glucose (Wang et al., 2023). This difference might be attributed to culture conditions, such as culture temperature, media, and selection plasmids.

Researchers in the field of metabolic engineering have adopted various strategies to expand the productivity of 2PE. The selection of genes related to the biosynthetic pathway of 2PE, optimization of gene expression, culture systems such as co-cultures using multiple strains, and the exploration of alternative pathways have been carried out previously (Wang et al., 2019; Zhan et al., 2022; Rao et al., 2023). However, to the best of our knowledge, there are no reports of 2PE production using an enzymatic-engineering approach in the biosynthesis pathway.

3.3. Designing ARO10 mutants to increase the production of 2PE

Computer-aided rational design of enzymes can help improve their desired functions, and several studies attempting to increase the yield and amount of target compounds using tailored enzymes have been reported (Machado et al., 2012; Mori et al., 2021; Gao et al., 2022). To date, the crystal structure of ARO10 derived from *S. cerevisiae* has not been reported. Thus, we first performed homology modeling of ARO10 using the crystal structure of pyruvate decarboxylase derived from *S. cerevisiae* (PDB: 2VK8, 36.2 % identity, 54.4 % similarity). The final models of ARO10 showed reasonable stereochemistry, with 95.1 % of residues located in the favored regions of the Ramachandran plot. Only two residues (S60 and V361) were found in outlier regions. The quality of the ARO10 structural model was estimated to be 0.68 ± 0.05 using the global error scoring functions QMEANDisCo (https://swissmodel.expasy.org/qmean/). ARO10 forms a homodimer, and each subunit contains a ThDP cofactor, which mediates the decarboxylation of 2-keto acid substrates (Kneen et al., 2011). In the generated homology model of ARO10, ThDP and phenylpyruvate are located at the interface between subunits A and B (Fig. 4a). The model of phenylpyruvate-bound ARO10 showed that D49 and H144 (subunit A) interacted with the carboxylate group of phenylpyruvate, and H145 (subunit A) interacted with its keto group. ARO10 decarboxylation requires ThPD, D49, H144, and H145, and the substrate specificity of ARO10 is determined by residues surrounding subunit B at the substrate-binding site. In the substrate-binding site of ARO10, hydrophobic amino acid residues (V289, M290, I335, T444, F449, L469, I544, I548, L621, V625, and A628) and two hydrophilic amino acid residues (N307 and E334) were located a short distance away, clustered, and formed large cavities; this might explain why ARO10 showed broad substrate specificity but tended to accept larger substrates. For example, the activity of phenylpyruvate is 100 %, and that of pyruvate is 0.2 % (Kneen et al., 2011).

To improve the decarboxylation of phenylpyruvate via ARO10, an amino acid substitution was performed at the ARO10 substrate-binding site. This substitution would stabilize the aromatic ring of phenylpyruvate while maintaining the amino acid residues (D49, H144, and H145) involved in binding to the 2-keto acid group. We generated single-substitution mutants *in silico* and arranged them in the order of the affinity improvement factor for phenylpyruvate, after which we produced good designs of ARO10 mutants and investigated their activity (Fig. 4b). As a result of *in vivo* screening of $C3A10_{mut}yk$ and CFT3 strains harboring the ARO10 mutant and yahk, several mutants showed an improvement in 2PE production, and the best design, ARO10 I544W, achieved a 4.1-fold enhancement.

In vitro enzyme assays were conducted to gain insight into the mechanism of increased activity displayed by the ARO10 I544W variant. Kinetic studies of the ARO10 I544W determined that the K_m and V_{max} values are 1.23 mM and 2.42×10^{-4} mM/s, respectively (Fig. 5A). When compared to the kinetic parameters of ARO10 WT ($K_m = 1.23$ mM and $V_{max} = 1.82 \times 10^{-4}$ mM/s), the I544W mutation resulted in an increase in V_{max} while maintaining K_m. Interestingly, the enzymatic activity *in vivo* showed a greater enhancement compared to that observed *in vitro*, with a 4.1-fold increase *in vivo* and a 1.3-fold increase *in vitro*, respectively. The volume of the substrate-binding site in enzymes is related to the breadth of substrate specificity. By comparing the simulated active site of WT and I544W, it was observed that the I544W substitution made the hydrophobic cavity in the substrate-binding site smaller (Fig. 5B and C). In addition to phenylpyruvate, numerous other 2-keto acid metabolites are present within cells. Therefore, the I544W mutation might enhance ARO10 activity *in vivo* due to the restriction of compounds entering the pocket. By employing rational design based on *in silico* calculations, the best ARO10 mutant, ARO10 I544W, was obtained with

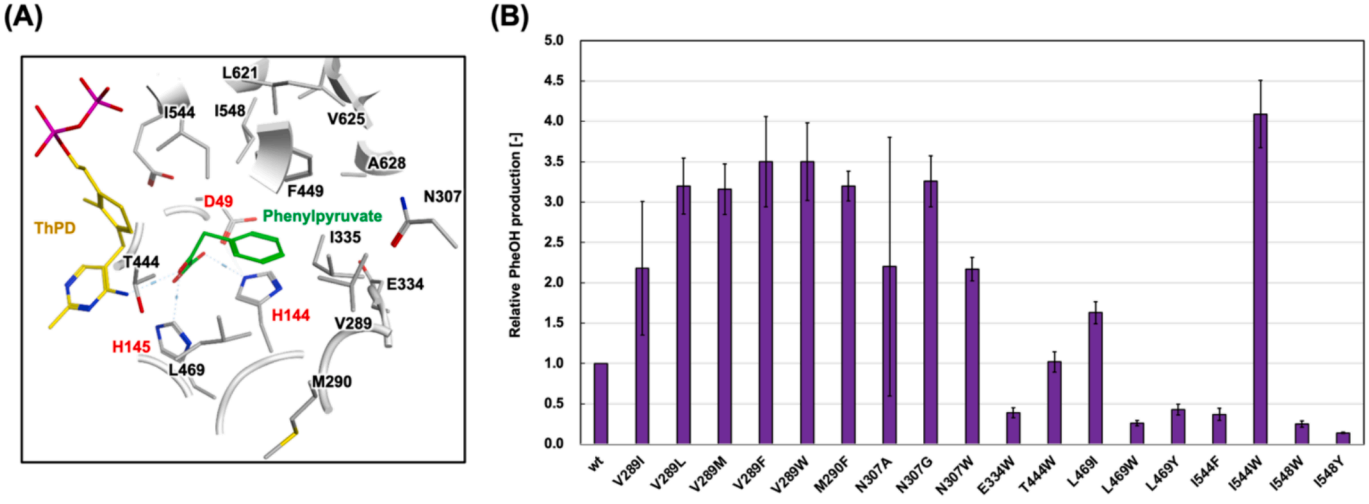

Fig. 4. Design of the ARO10 mutant for 2PE production. (a) Homology model of the active site of ARO10 with phenylpyruvate (light green) and ThDP from PDB:2Q5O with the lowest energy poses. The negative hydrogen network and hydrophobic interactions are indicated by dashed lines. (b) Relative 2PE productivity of CFT3 harboring ARO10 mutants. The productivity of CFT3 harboring ARO10 WT (ARO10 was defined as 1). Data are presented as the mean ± standard deviation of three independent experiments. (For interpretation of the references to colour in this figure legend, the reader is referred to the web version of this article.)

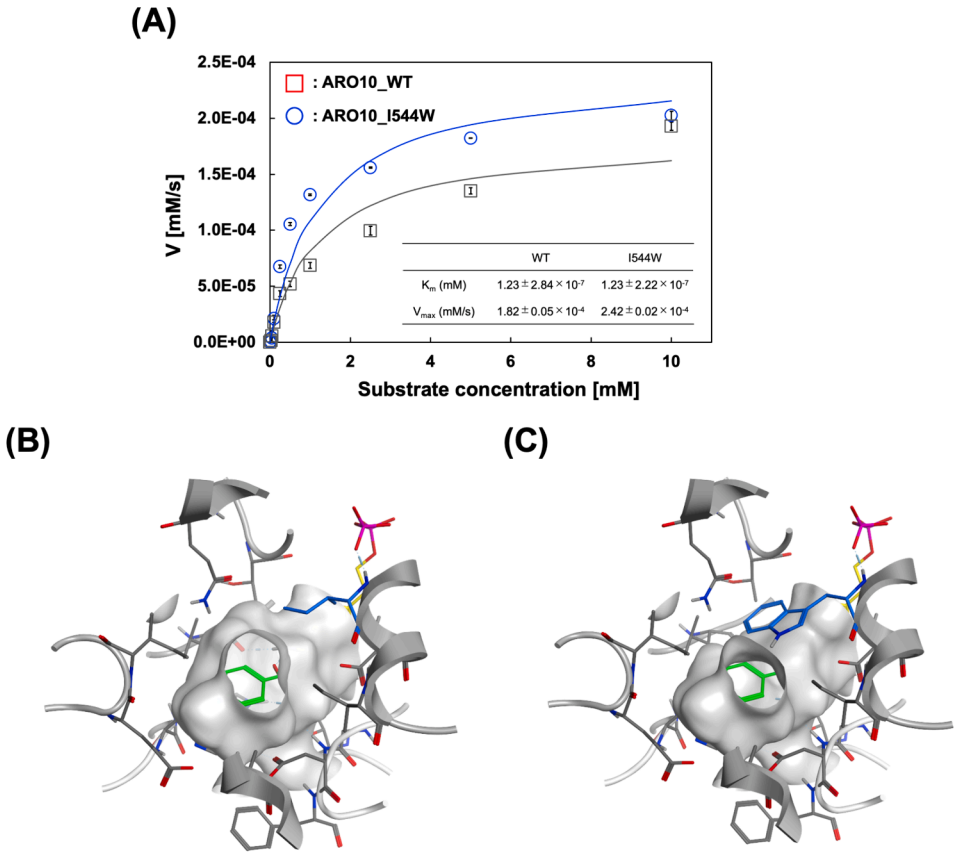

Fig. 5. Simulated active site of ARO10. (a) WT and (b) I544W mutant. Protein surface of the substrate-binding site within 4.5 Å from phenylpyruvate is shown in white.

a small library size of mutants.

3.4. 2PE production in CFT3 expressing $ARO10_{I544W}$ mutant and YahK from e. Coli

Finally, we produced 2PE using CFT3 expressing the $ARO10_{I544W}$

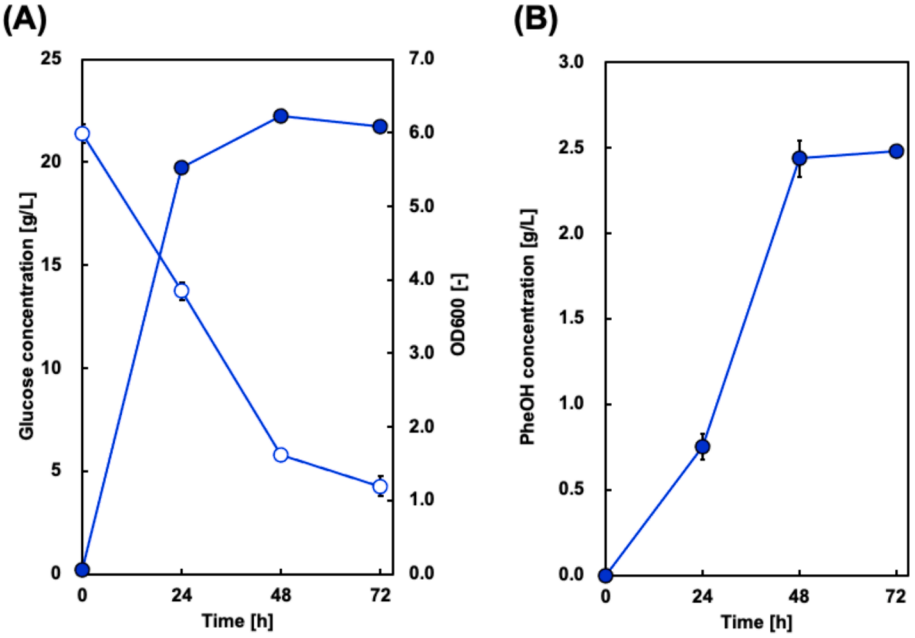

Fig. 6. Culture profiles of the 2PE-producing strain, which expresses $ARO10_{I544w}$ and yahK. Time course of (a) OD_{600} values (open symbols) and the amount of consumed glucose (closed symbols), and (b) the amount of 2PE produced by $C3A10_{I544W}yk$. Data are presented as the mean ± standard deviation of three independent experiments.

mutant and YahK. Fig. 6 shows the culture profile of C3A10$_{I544W}$yk. The amount of 2PE produced and yield from glucose reached 2.5 g/L and 0.16 g/g, respectively, after 72 h of cultivation. The amount of produced 2PE and consumed glucose in C3A10$_{I544W}$yk were higher and almost 2-fold higher than those of C3HA10yk, respectively. The 2PE titer was the highest among previous reports investigating 2PE production using *E. coli* as the host strain (Table S3). Although the maximal amount of produced 2PE was achieved using *B. licheniformis*, to the best of our knowledge, the yield from glucose achieved in this study is the highest (Table S3; Rao et al., 2023).

In the 2PE-producing strains created here, NADPH was mainly generated in the pentose phosphate pathway (PPP) because the parental strain CFT3 is a Phe producer whose intracellular availability of erythrose-4-phosphate (E4P) is enhanced, and PPP is assumed to be active. Within the PPP in *E. coli*, zwf and gnd, which encode glucose-6-phosphate 1-dehydrogenase and 6-phosphogluconate dehydrogenase, respectively, are involved in the generation of NADPH. The accumulation of intracellular concentrations of NADH or NADPH is known to impair microbial growth, whereas the redox balance of coenzymes is one of the most important factors in determining the microbial production of bulk chemicals (Liang and Shen, 2017; Noda et al., 2019; Yuan et al., 2022). In the 2PE biosynthesis pathway, ALR, which catalyzes the conversion of phenylacetaldehyde into 2PE, consumes 1 mol of NADH or NADPH to produce 1 mol of 2PE. YahK, which we adopted here, prefers NADPH to NADH, although its activity toward NADH and the details of its actual selectivity between NADPH and NADH have not yet been investigated (Pick et al. (2013)). In this study, the use of ARO10$_{I544W}$ promotes the formation of phenylacetaldehyde, and NADPH produced in the PPP is consumed by YahK to synthesize 2PE. These results correspond to the higher consumption of glucose and higher yield of 2PE in C3A10$_{I544W}$yk than those in C3HA10yk.

During the 2PE production from glucose using genetically engineered *E. coli*, the amount of produced 2PE was approximately 1 g/L, with a glucose yield below 0.1 g/g. Machas et al. (2017) demonstrated the production of 2PE using an alternative biosynthetic pathway derivative from styrene synthesis. This novel route to 2PE has an approximately 10-fold greater thermodynamic driving force than that of the Ehrlich pathway. The amount of 2PE produced reached 1.94 g/L, although the yield from glucose was 0.06 g/g, showing the novel pathway is a promising route to produce 2PE. In contrast, Wang et al. (2023) reported the opposite result by comparing styrene-derived and Ehrlich pathways in a base strain with the same genotype. In their report, 2PE production was performed using *ARO10* and *yjgB*-expressing *E. coli* dependent on the Ehrlich pathway. The amount of produced 2PE reached 2.28 g/L, while the yield from glucose was 0.076 g/g. Developing a co-culture system that includes *M. guilliermondii* has successfully increased the production of 2PE using *E. coli* to 3.77 g/L. This was achieved even though the yield from glucose stood at 0.05 g/g, and *E. coli* primarily served as the Phe producer (Yan et al., 2022).

4. Conclusion

In the present study, we enhanced the production of 2PE using engineered *E. coli* strains. The strategy for metabolic engineering was to optimize the plasmid vector and select a suitable ALR in combination with *ARO10* as the PDC. To enhance the production of 2PE, we focused on the *ARO10* evolution. Using rational enzyme design based on *in silico* computational simulations, ARO10 mutants were evaluated for their 2PE production. Using the ARO10 I544W mutant-expressing *E. coli*, the maximum amount of 2PE produced detected in the culture broth reached 2.5 g/L, and the yield from glucose was 0.16 g/g. To the best of our knowledge, these are the highest 2PE production values reported for a batch culture of *E. coli* as the host strain. However, the titer of 2PE produced has not reached the level produced using *B. licheniformis* as a host strain, whereas the yield from glucose was comparable to that produced using *B. licheniformis*. In addition, double ARO10 mutants with promising 2PE production yields have not yet been generated. To enhance 2PE productivity, future efforts should focus on integrating strategies such as the engineering of ARO10 and YahK enzymes, scaling up the culture process, and implementing fed-batch cultivation.

Funding

This work has been supported by the RIKEN Center for Sustainable Resource Science (to S.N., Y.M., R.F., M.D., T.S., and A.K.), by Japan Science and Technology Agency (JST) through the JST-Mirai Program (Grant Number JPMJMI17EI to S.N., R.F., and Y.M.) and the Precursory Research for Embryonic Science and Technology (PRESTO) grant number JPMJPR22N9 (to S.N.), by the Special Postdoctoral Researcher Program (to S.N.), by JSPS KAKENHI Grant Number 22H01885 (to S.N.) and 23H04565 (to S.N.), and by the FY2018, FY2020, and FY2022 Incentive Research Projects (to N.S.).

CRediT authorship contribution statement

Shuhei Noda: Writing – review & editing, Writing – original draft, Visualization, Validation, Supervision, Resources, Project administration, Methodology, Investigation, Funding acquisition, Formal analysis, Data curation, Conceptualization. **Yutaro Mori:** Writing – review & editing, Writing – original draft, Visualization, Validation, Methodology, Investigation, Formal analysis, Data curation, Conceptualization. **Yuki Ogawa:** Writing – review & editing, Methodology, Investigation, Formal analysis. **Ryosuke Fujiwara:** Writing – review & editing, Methodology, Investigation, Formal analysis. **Mayumi Dainin:** Investigation, Formal analysis, Data curation. **Tomokazu Shirai:** Writing – review & editing, Methodology, Formal analysis, Data curation. **Akihiko Kondo:** Resources.

Declaration of competing interest

The authors declare that they have no known competing financial interests or personal relationships that could have appeared to influence the work reported in this paper.

Data availability

Data will be made available on request.

Acknowledgments

The authors would like to thank Editage (www.editage.jp) for the English language review.

Appendix A. Supplementary data

Supplementary data to this article can be found online at https://doi.org/10.1016/j.biortech.2024.130927.

References

Atsumi, S., Hanai, T., Liao, J.C., 2008. Non-fermentative pathways for synthesis of branched-chain higher alcohols as biofuels. Nature. 451, 86–89. https://doi.org/10.1038/nature06450.

Bloom, J.D., Meyer, M.M., Meinhold, P., Otey, C.R., Macmillan, D., Arnold, F.H., 2005. Evolving strategies for enzyme engineering. Curr. Opin. Struct. Biol. 15, 447–452. https://doi.org/10.1016/j.sbi.2005.06.004.

Chen, X., Wang, Z., Guo, X., Liu, S., He, X., 2017. Regulation of general amino acid permeases Gap1p, GATA transcription factors Gln3p and Gat1p on 2-phenylethanol biosynthesis via Ehrlich pathway. J. Biotechnol. 242, 83–91. https://doi.org/10.1016/j.jbiotec.2016.11.028.

Choi, K.R., Jiao, S., Lee, S.Y., 2020. Metabolic engineering strategies toward production of biofuels. Curr. Opin. Chem. Biol. 59, 1–14. https://doi.org/10.1016/j.cbpa.2020.02.009.

Crawshaw, R., Crossley, A.E., Johannissen, L., Burke, A.J., Hay, S., Levy, C., Baker, D., Lovelock, S.L., Green, A.P., 2022. Engineering an efficient and enantioselective

enzyme for the Morita–Baylis–Hillman reaction. Nat. Chem. 14, 313–320. https://doi.org/10.1038/s41557-021-00833-9.
Feng, H., Wang, H.-Y., Zhao, H.-Y., 2017. Novel Random Mutagenesis Method for Directed Evolution, pp. 483–490. https://doi.org/10.1007/978-1-4939-6472-7_32.
Gao, J., Du, M., Zhao, J., Zhang, Y., Xu, N., Du, H., Ju, J., Wei, L., Liu, J., 2022. Design of a genetically encoded biosensor to establish a high-throughput screening platform for L-cysteine overproduction. Metab. Eng. 73, 144–157. https://doi.org/10.1016/j.ymben.2022.07.007.
Gu, Y., Ma, J., Zhu, Y., Xu, P., 2020. Refactoring Ehrlich pathway for high-yield 2-phenylethanol production in *Yarrowia lipolytica*. ACS Synth. Biol. 9, 623–633. https://doi.org/10.1021/acssynbio.9b00468.
Hua, D., Xu, P., 2011. Recent advances in biotechnological production of 2-phenylethanol. Biotechnol. Adv. 29, 654–660. https://doi.org/10.1016/j.biotechadv.2011.05.001.
Jovanovic, S., Dietrich, D., Becker, J., Kohlstedt, M., Wittmann, C., 2021. Microbial production of polyunsaturated fatty acids — high-value ingredients for aquafeed, superfoods, and pharmaceuticals. Curr. Opin. Biotechnol. 69, 199–211. https://doi.org/10.1016/j.copbio.2021.01.009.
Kneen, M.M., Stan, R., Yep, A., Tyler, R.P., Saehuan, C., McLeish, M.J., 2011. Characterization of a thiamin diphosphate-dependent phenylpyruvate decarboxylase from *Saccharomyces cerevisiae*. FEBS Journal. 278, 1842–1853. https://doi.org/10.1111/j.1742-4658.2011.08103.x.
Koma, D., Yamanaka, H., Moriyoshi, K., Ohmoto, T., Sakai, K., 2012. Production of aromatic compounds by metabolically engineered *Escherichia coli* with an expanded shikimate pathway. Appl. Environ. Microbiol. 78, 6203–6216. https://doi.org/10.1128/AEM.01148-12.
Li, R., Wijma, H.J., Song, L., Cui, Y., Otzen, M., Tian, Y., Du, J., Li, T., Niu, D., Chen, Y., Feng, J., Han, J., Chen, H., Tao, Y., Janssen, D.B., Wu, B., 2018. Computational redesign of enzymes for regio- and enantioselective hydroamination. Nat. Chem. Biol. 14, 664–670. https://doi.org/10.1038/s41589-018-0053-0.
Liang, K., Shen, C.R., 2017. Selection of an endogenous 2,3-butanediol pathway in *Escherichia coli* by fermentative redox balance. Metab. Eng. 39, 181–191. https://doi.org/10.1016/j.ymben.2016.11.012.
Lu, H., Villada, J.C., Lee, P.K.H., 2019. Modular metabolic engineering for biobased chemical production. Trends Biotechnol. 37, 152–166. https://doi.org/10.1016/j.tibtech.2018.07.003.
Machado, H.B., Dekishima, Y., Luo, H., Lan, E.I., Liao, J.C., 2012. A selection platform for carbon chain elongation using the CoA-dependent pathway to produce linear higher alcohols. Metab. Eng. 14, 504–511. https://doi.org/10.1016/j.ymben.2012.07.002.
Machas, M.S., McKenna, R., Nielsen, D.R., 2017. Expanding upon styrene biosynthesis to engineer a novel route to 2-phenylethanol. Biotechnol. J. 12 https://doi.org/10.1002/biot.201700310.
Mori, Y., Noda, S., Shirai, T., Kondo, A., 2021. Direct 1,3-butadiene biosynthesis in *Escherichia coli* via a tailored ferulic acid decarboxylase mutant. Nat. Commun. 12, 2195. https://doi.org/10.1038/s41467-021-22504-6.
Nielsen, J., 2019. Yeast systems biology: model organism and cell factory. Biotechnol. J. 14, e1800421.
Noda, S., Mori, Y., Oyama, S., Kondo, A., Araki, M., Shirai, T., 2019. Reconstruction of metabolic pathway for isobutanol production in *Escherichia coli*. Microb. Cell Factories. 18, 124. https://doi.org/10.1186/s12934-019-1171-4.
Otero-Muras, I., Carbonell, P., 2021. Automated engineering of synthetic metabolic pathways for efficient biomanufacturing. Metab. Eng. 63, 61–80. https://doi.org/10.1016/j.ymben.2020.11.012.
Park, R., Ongpipattanakul, C., Nair, S.K., Bowers, A.A., Kuhlman, B., 2023. Designer installation of a substrate recruitment domain to tailor enzyme specificity. Nat. Chem. Biol. 19, 460–467. https://doi.org/10.1038/s41589-022-01206-0.
Pick, A., Rühmann, B., Schmid, J., Sieber, V., 2013. Novel CAD-like enzymes from *Escherichia coli* K-12 as additional tools in chemical production. Appl. Microbiol. Biotechnol. 97, 5815–5824. https://doi.org/10.1007/s00253-012-4474-5.
Rao, Y., Wang, J., Yang, X., Xie, X., Zhan, Y., Ma, X., Cai, D., Chen, S., 2023. A novel toolbox for precise regulation of gene expression and metabolic engineering in *Bacillus licheniformis*. Metab. Eng. 78, 159–170. https://doi.org/10.1016/j.ymben.2023.06.004.
Vuralhan, Z., Morais, M.A., Tai, S.L., Piper, M.D.W., Pronk, J.T., 2003. Identification and characterization of phenylpyruvate decarboxylase genes in *Saccharomyces cerevisiae*. Appl. Environ. Microbiol. 69, 4534–4541. https://doi.org/10.1128/AEM.69.8.4534-4541.2003.
Vuralhan, Z., Luttik, M.A.H., Tai, S.L., Boer, V.M., Morais, M.A., Schipper, D., Almering, M.J.H., Kötter, P., Dickinson, J.R., Daran, J.M., Pronk, J.T., 2005. Physiological characterization of the ARO10-dependent, broad-substrate-specificity 2-oxo acid decarboxylase activity of *Saccharomyces cerevisiae*. Appl. Environ. Microbiol. 71, 3276–3284. https://doi.org/10.1128/AEM.71.6.3276-3284.2005.
Wang, Z., Bai, X., Guo, X., He, X., 2017b. Regulation of crucial enzymes and transcription factors on 2-phenylethanol biosynthesis via Ehrlich pathway in *Saccharomyces cerevisiae*. J. Ind. Microbiol. Biotechnol. 44, 129–139. https://doi.org/10.1007/s10295-016-1852-5.
Wang, Z., Jiang, M., Guo, X., Liu, Z., He, X., 2018. Reconstruction of metabolic module with improved promoter strength increases the productivity of 2-phenylethanol in *Saccharomyces cerevisiae*. Microb. Cell Factories. 17, 60. https://doi.org/10.1186/s12934-018-0907-x.
Wang, G., Wang, M., Yang, J., Li, Q., Zhu, N., Liu, L., Hu, X., Yang, X., 2023. De novo synthesis of 2-phenylethanol from glucose by metabolically engineered *Escherichia coli*. J. Ind. Microbiol. Biotechnol. 49 https://doi.org/10.1093/jimb/kuac026.
Wang, P., Yang, X., Lin, B., Huang, J., Tao, Y., 2017a. Cofactor self-sufficient whole-cell biocatalysts for the production of 2-phenylethanol. Metab. Eng. 44, 143–149. https://doi.org/10.1016/j.ymben.2017.09.013.
Wang, Y., Zhang, H., Lu, X., Zong, H., Zhuge, B., 2019. Advances in 2-phenylethanol production from engineered microorganisms. Biotechnol. Adv. 37, 403–409. https://doi.org/10.1016/j.biotechadv.2019.02.005.
Weise, N.J., Parmeggiani, F., Ahmed, S.T., Turner, N.J., 2015. The bacterial ammonia lyase EncP: a tunable biocatalyst for the synthesis of unnatural amino acids. J. Am. Chem. Soc. 137, 12977–12983. https://doi.org/10.1021/jacs.5b07326.
Yan, W., Gao, H., Jiang, W., Jiang, Y., Lin, C.S.K., Zhang, W., Xin, F., Jiang, M., 2022. The de novo synthesis of 2-phenylethanol from glucose by the synthetic microbial consortium composed of engineered *Escherichia coli* and *Meyerozyma guilliermondii*. ACS Synth. Biol. 11, 4018–4030. https://doi.org/10.1021/acssynbio.2c00368.
Yuan, S.F., Nair, P.H., Borbon, D., Coleman, S.M., Fan, P.H., Lin, W.L., Alper, H.S., 2022. Metabolic engineering of *E. coli* for β-alanine production using a multi-biosensor enabled approach. Metab. Eng. 74, 24–35. https://doi.org/10.1016/j.ymben.2022.08.012.
Zhan, Y., Shi, J., Xiao, Y., Zhou, F., Wang, H., Xu, H., Li, Z., Yang, S., Cai, D., Chen, S., 2022. Multilevel metabolic engineering of Bacillus licheniformis for de novo biosynthesis of 2-phenylethanol. Metab. Eng. 70, 43–54. https://doi.org/10.1016/j.ymben.2022.01.007.
Zhu, N., Xia, W., Wang, G., Song, Y., Gao, X., Liang, J., Wang, Y., 2023. Engineering *Corynebacterium glutamicum* for de novo production of 2-phenylethanol from lignocellulosic biomass hydrolysate. Biotechnol. Biofuels Bioprod. 16, 75. https://doi.org/10.1186/s13068-023-02327-x.
Zhu, L., Xu, S., Li, Y., Shi, G., 2021. Improvement of 2-phenylethanol production in *Saccharomyces cerevisiae* by evolutionary and rational metabolic engineering. PLOS ONE. 16, e0258180.